

## GLOBAL JOURNAL OF ENGINEERING SCIENCE AND RESEARCHES SINGLE AND TWO STAGE INVERTER BASED GRID CONNECTED PHOTOVOLTAIC POWER PLANT WITH RIDE THROUGH CAPABILITY UNDER GRID FAULTS

K Mounika<sup>1</sup>, V Satya Devi<sup>2</sup>, K Jaya Prakash<sup>3</sup> & M Uday Kumar<sup>4</sup>  
\*<sup>1,2,3&4</sup> Student, EEE Department, Pragati Engineering college, India

### ABSTRACT

Grid-connected PV systems will become an even active player in the future mixed power systems, which are linked by a vast of power electronics converters. In order to achieve a reliable and efficient power generation from PV systems, stringent demands have been imposed on the entire PV system. In this project, the control of VSIs used in single and two-stage grid-connected photo voltaic (PV) power plants is developed to address the issue of inverter disconnecting under various grid faults. Inverter control incorporates reactive power support in the case of voltage sags based on the grid codes' (GCs) requirements to ride-through the faults and support the grid voltages.

A case study of 1-MW system simulated in MATLAB/Simulink software is used to illustrate the proposed control. Problems that occur during grid faults along with associated remedies are being discussed. The voltage and current comparison for single stage and two stage inverter under grid faults are presented in the MATLAB/Simulink platform. The proposed hybrid system will regulate dc-link voltage and supply reactive power to the grid. A smooth switching technique will be adopted to switch between normal mode to faulty mode and vice versa

**Keywords:** DC–DC converter, fault-ride-through, photovoltaic (PV) systems, power system faults, reactive power support

### I. INTRODUCTION

Researches so far shows that, by 2020, around 20% of the total energy production worldwide will be generated from renewable energy. But the major problem with the standalone system is that the sources are not continuous. This intermittent nature of the sources can tamper the power system stability.

Hence we can combine two or more such renewable energy sources to form a hybrid renewable energy system. Such hybrid systems are more promising and effective in generating power, especially in remote areas, as compared to individual systems. They could bring out the advantages of each renewable source being combined and also complement the demands of conventional power systems. There are so many renewable energy sources available, but Wind and solar power projects are widely getting implemented that they are of free access and environment – friendly. But for the connection of new generation systems into our existing grids, the transmission system operators define minimum requirements that should be met, which is called Grid Code. The major challenge with a grid connected hybrid system is that they must contribute with the power quality and power system stability. During a fault at the grid side, it's the voltage at the point of common coupling (PCC) which drops suddenly. This will adversely affects the entire hybrid system as the drop in voltage abruptly increases the rotor speed of the wind energy conversion system (WECS) generator and also affects the normal operation of the PV system. Thus, in order to protect the renewable systems, it was customary practice to disconnect the renewable systems upon faulty grid conditions. But, nowadays, due to higher penetration of renewable systems into the grid, disconnection of such a large number of renewable systems instantly from the grid during fault can aggravate the power system stability issues. Because removal of such large scale hybrid generation during voltage dip will further cause the voltage to go down, which in turn results in the disconnection of more generation units, leading to a cascading failure. Among several studies for unbalanced voltage sags, a method was introduced in [8] to mitigate the peak output currents of a 4.5-kVA PV system in non faulty phases. Another study in [9] presented a proportional-resonant (PR) current

controller for the current limiter to ensure sinusoidal output current waveforms and avoid over-current. However, in the mentioned studies, reactive power support was not considered. In [10], a study dealing with the control of the positive and negative sequences was performed. Two parallel controllers were implemented, one for each sequence. The study demonstrated the dynamic limitations of using this control configuration due to the delays produced in the current control loops. A study was reported in [11] for the control of the dc side of the inverter, which shows the impact of various types of faults on the voltage and current of the PV array. Considering FRT strategies for grid-connected VSIs, some research has been done on wind turbine applications [12]–[14] and also on VSI-based high-voltage direct current (HVDC) systems [15]–[17]. Some of these studies are based on passive control, e.g., crowbar and chopper resistors [14], [15], whereas others are based on active control schemes [12], [13], [16], [17]. Although both categories can provide FRT capability, the passive methods have the drawbacks of requiring additional components and dissipating significant power during the voltage sag processes. In the application of GCPPPs with the configurations of single-stage conversion (single-stage conversion means direct connection of the PV source to the dc side of the VSI), some research were done in [18] and [19] evaluating the FRT issues of both ac and dc sides of the inverter under unbalanced voltage conditions. However, in the application of a two-stage conversion (meaning a dc–dc conversion or preregulator unit exists between the PV source and VSI). PV inverter disconnection under grid faults occurs due to mainly three factors: 1) excessive dc-link voltage; 2) excessive ac currents; and 3) loss of grid voltage synchronization, which may conflict with the FRT capability.

In this paper, the control strategy introduced in [18] for a single-stage conversion is used, although the voltage sag detection and reactive power control is modified based on individual

measurements of the grid voltages. The main objective of this paper is to introduce new control strategies for the twostage conversion in GCPPPs that allow the inverter to remain connected to the grid under various types of faults while injecting reactive power to meet the required GCs. Some selected simulation results for single- and two-stage configurations are presented to confirm the effectiveness of the proposed control strategies.

## II. DEMANDS FOR GRID-CONNECTED PHOTOVOLTAIC SYSTEMS

The grid-connected PV systems are being developed at a very fast rate and will soon take a major part of power electricity generation in some areas [22], [23]. At the same time, the demands (requirements) to the PV systems as shown Fig. 2 are becoming much tougher than ever before. Although the power capacity of a PV system currently is still not comparable to that of an individual wind turbine system, similar demands to wind turbine systems are being transitioned to the PV systems [18], [21], since the number of large-scale PV systems (power plants) is continuously increased [24]

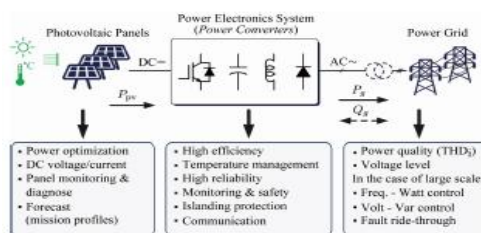


Fig. 2. Demands (challenges) for a grid-connected PV system based on power electronics converters. Nevertheless, the demands for PV systems can be specified at different levels. At the PV side, the output power of the PV panels/strings should be maximized, where a DCDC converter is commonly used, being a double-stage PV system. This is known as the Maximum Power Point Tracking (MPPT). In this case, the DC voltage (DC-link voltage) should be maintained as a desirable value for the inverter. Moreover, for safety (e.g., fire), the panel monitoring and diagnosis have to be enhanced at the PV side [25]. At the grid side, normally a desirable Total Harmonic Distortion (THD) of the output current should be attained (e.g., lower than 5%) [26]. In the case of large-scale PV systems with higher power ratings, the PV systems should not violate the grid voltage and the grid frequency by means of providing ancillary services (e.g., frequency regulation).

Additionally, the PV systems have to ride-through grid faults (e.g., voltage sags and frequency changes), when a higher PV penetration level comes into reality [18], [21], [27]-[33].

**III. POWER CONVERTER TOPOLOGY FOR SINGLE STAGE PV SYSTEM:**

Each of the grid-connected concepts consists of series of paralleled PV panels or strings, and they are configured by a couple of power electronics converters (DC-DC converters and DC-AC inverters) in accordance to the output voltage of the PV panels as well as the power rating.

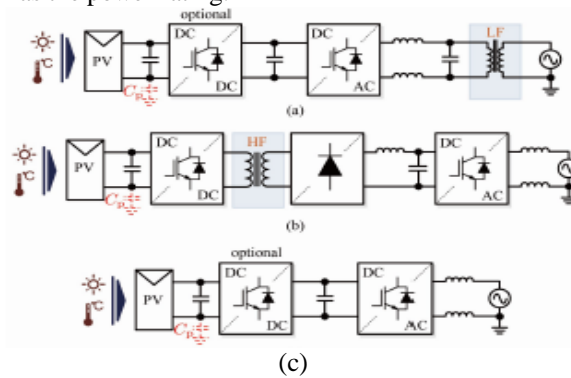


Fig. Single-phase grid-connected PV systems, where the AC-module inverters, the string inverters, and the multi-string inverters are commonly used: (a) with a low-frequency (LF) transformer, (b) with a high frequency (HF) transformer, and (c) without transformers. Traditionally, an isolation transformer can be adopted either at the grid-side with low frequencies or as a high frequency transformer in such PV converters, as it is shown in Fig. (a) and (b). Both grid-connected PV technologies are available on the market with an overall efficiency of 93-95% [26], to which is mainly contributed by the bulky transformers.

**Case study system specifications**

PV module specifications		PV inverter specifications	
Maximum operating voltage ( $V_{mpp}$ )	35.6 V	Maximum dc power	1133 kW
Maximum operating current ( $I_{mpp}$ )	8.29 A	Maximum dc input voltage	1000 V
Open circuit voltage ( $V_{oc}$ )	44.3 V	Rated dc voltage	800 V
Short circuit current ( $I_{sc}$ )	8.74 A	Apparent power rating (at STC)	1100 kVA
Number of parallel modules, $n_p$	155	<b>Filter</b>	$R = 1\text{ m}\Omega$ $L = 150\ \mu\text{H}$
Number of series modules, $n_s$	22	<b>Transformer</b>	1.2 MVA 20/0.415 kV Dyn11 50 Hz

In order to increase the overall efficiency, a vast of transformerless PV converters have been developed. Transformerless structures are mostly derived from the full bridge topology by providing an AC path or a DC path using additional power switching devices.

This will result in an isolation between the PV modules and the grid during the zero-voltage states, thus leading to a low leakage current injection.

In concerning the FRT capability, the inverter disconnection factors are illustrated according to the GCs.

#### A. Grid Voltage Synchronization:

In grid-connected inverters, one important issue is the voltage phase angle detection. This is usually performed by phaselocked- loop (PLL) technique based on a synchronous reference frame PLL (SRF-PLL) [25], known as conventional PLL. The conventional PLL configuration does not perform well under unbalanced voltage sags and consequently may lead to the inverter being disconnected from the grid. So, the method based on moving average filters (MAFs) introduced is applied, which was also used in showing very satisfactory performance.

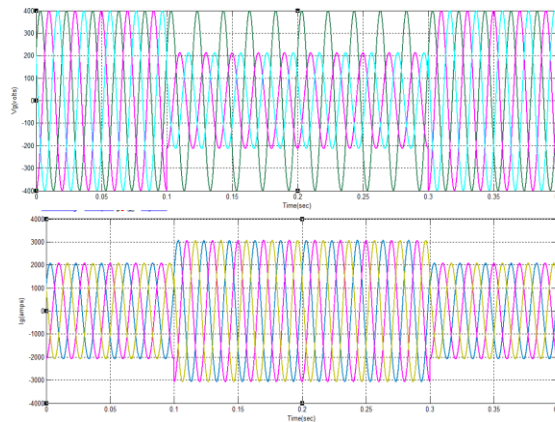


*Fig. 3. (a) Grid voltages and (b) grid currents at the LV side under 60% SLG voltage sag produced at MV side of the transformer.*

#### B Excessive AC Current:

Commercial grid-connected inverters have a maximum ac current value specified. If any of the currents exceed such value, the inverter is disconnected from the grid. Under a grid voltage sag, the  $d$ -component of the current (in the SRF) increases because the controller wants to maintain the active power injected into the grid and grid voltages are temporarily reduced.

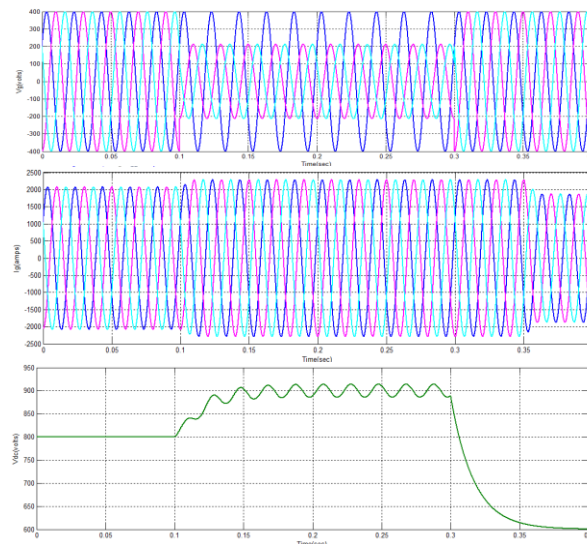


*Fig. 5. Adding the current limiter to the VSI control: (a) grid voltages; (b) grid currents; and (c) dc-link voltage under an SLG-voltage sag at MV side of the transformer*

Fig. 5 shows the generated currents after applying the current limiter in this example. One can observe in Fig. 5(b) that the grid currents are balanced. This is because the active current reference ( $i_{dref}$ ) is limited to an almost constant

value during the voltage sag. It should be mentioned that when operating with low solar radiation and/or small voltage sags, the active current reference may not be limited and therefore, it goes through the current limiter without being affected, i.e.,  $i_{dref} = I'_{dref}$ . As a consequence, if the voltage sag was unbalanced, the active current reference and consequently the output currents would contain some low-frequency harmonics.

**C Excessive DC-Link Voltage:**

In a single-stage GCPPP, as the dc-link voltage increases, the operating point on the  $I-V$  curve of PV array moves toward the open-circuit voltage point ( $V_{oc}$ ), which leads the PV current to decrease. The power generated by the PV panels is reduced because the operating point is taken away from the maximum power point (MPP) and therefore, less active current is injected into the ac side. This happens until the GCPPP reaches a new steady state where the dc-link voltage stops increasing.

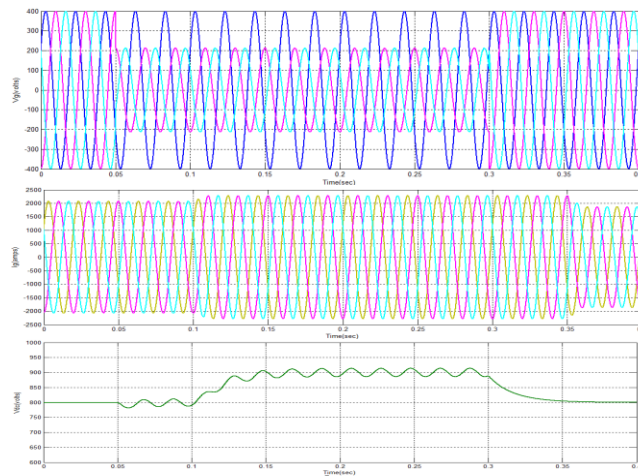


Fig. 8. Application of an anti-wind-up technique to the PI controller: (a) grid voltages; (b) grid currents; and (c) dc-link voltage under 60% SLG voltage sag at MV side of the transformer.

Control strategy:

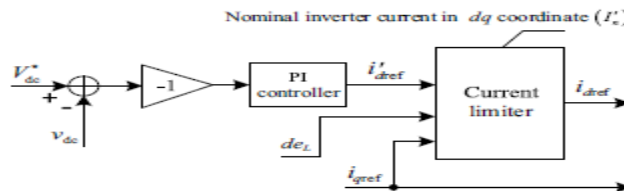


Fig. 4. Control diagram of the current limiter.

The positive sequence of the voltage is extracted from the grid by means of an ideal low-pass filter. Then, the angle of the positive sequence is detected.

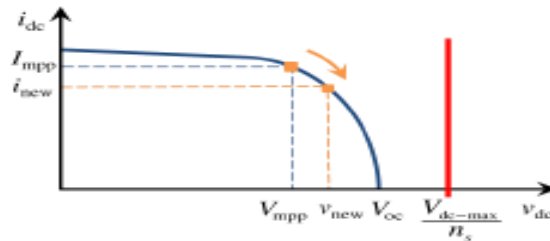


Fig. 6. Change in the PV operating point under voltage sag and maximum acceptable dc-link voltage.

The power generated by the PV panels is reduced because the operating point is taken away from the maximum power point (MPP) and therefore, less active current is injected into the ac side. This happens until the GCPPP reaches a new steady state where the dc-link voltage stops increasing. Thus, single-stage GCPPPs are self-protected because the generated power is reduced when the dc-link voltage increases under ac faults. It should be mentioned that the inverter has to withstand the worst case of the dc-link voltage, which is produced when the voltage provided by the PV modules reaches the open-circuit value ( $V_{oc}$ ) under the maximum solar radiation expected on the generation site.

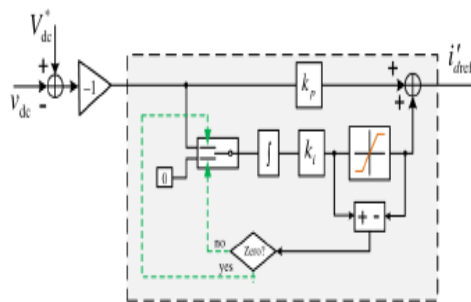


Fig. 7. PI controller with an anti-wind-up technique.

When the voltage sag ends, the excessive control action accumulated in the integral part of the controller has to be compensated by an input error in the opposite direction. As a consequence, the dc-link voltage is reduced below the reference value. In this case, a significant decrease of the dc-link voltage may lead to inverter losing control and be disconnected. To overcome this issue, an anti-wind-up technique is applied to stop the PI controller accumulating excessive control action when it exceeds a specified value [30]. The schematic of the anti-wind-up technique is shown in Fig. 7 in which  $V^*_{dc}$  and  $v_{dc}$  are the reference and actual dc-link voltages, respectively. The improved results when applying the anti-wind-up technique. In this case, once the grid fault is cleared, the dclink voltage recovers to the pre-fault value with no perceptible overcompensation.

Power Converter Topology for Two Stage PV System:

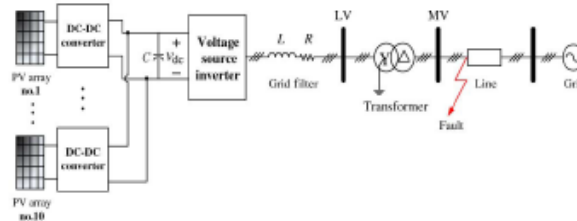


Fig. 9. Diagram of the two-stage conversion-based GCPPP

A two-stage GCPPP includes a dc–dc converter between the PV arrays and the inverter. In high-power GCPPPs, more than one dc–dc converter can be included, one per each PV array. Despite having several dc–dc converters,

these systems will be referred anyway as two-stage GCPPPs. In two-stage GCPPPs, the MPP tracking (MPPT) is performed by the dc–dc converter and the dc-link voltage is regulated by the inverter.

During a voltage sag, if no action is taken in the control of the dc–dc converter, the power from the PV modules is not reduced and therefore, the dc-link voltage keeps rising and may exceed the maximum limit. Hence, the system is not self-protected during grid fault conditions. A specific control action has to be taken to reduce the power generated by the PV modules and provide the two-stage GCPPP with FRT capability.

TABLE II PV ARRAYS AND DC–DC CONVERTER SPECIFICATIONS IN TWO-STAGE GCPPP

DC–DC converter and PV array specifications			
Input voltage of the dc–dc converter at MPP, $V_{pv}$	356 V	Output voltage of the dc–dc converter, $V_{dc}$	800 V
Number of parallel PV modules in each array, $n_p$	34	DC–DC converter inductance, $L_i$	1 mH
Number of series PV modules in each array, $n_s$	10	DC-link capacitance, $C$	31 mF

A feed-forward strategy is applied to improve the dynamics of the dc-link voltage. The strategy is based on the assumption that the PV generated power is equal to the injected power into the grid, i.e.,

$$i_{pv}v_{pv} = e_d i_d + e_q i_q \tag{4}$$

where  $i_{pv}$  and  $v_{pv}$  are the PV current and voltage, respectively, and  $e_d$  and  $e_q$  are the  $d$  and  $q$  grid voltage components extracted by the PLL. Since the PLL forces the  $e_q$  component to be zero, the estimated  $d$  current component is obtained as

$$i_{d-est} = \frac{i_{pv}v_{pv}}{e_d} \tag{5}$$

In two-stage GCPPPs, three different ways to limit the dc-link voltage under fault conditions are proposed: 1) shortcircuiting the PV array by turning ON the switch of the dc–dc converter throughout the voltage sag duration; 2) leaving the PV array open by turning OFF the switch of the dc–dc converter; and 3) changing the control of the dc–dc converter to inject less power from the PV arrays when compared with the pre-fault operating conditions. It should be mentioned that in all the configurations including single-stage conversion, the MPPT is disabled during the voltage sag condition and the voltage reference of pre-fault condition ( $V_{mpp}$ ) is considered. Once the fault ends, the MPPT is reactivated. In the two-stage topology, the first two solutions explained next stop transferring energy from the PV arrays to the dc bus, whereas the dc bus keeps regulated at the reference value by the voltage control loop. In the third method, the MPPT is disconnected and the PV operating point moves to a lower power level to avoid overvoltage in the dc-link.

Therefore, no matter the MPPT technique is voltage or current controlled and the algorithms implemented for the MPPT, the performance of the proposed methods during the voltage sag condition remains the same because the MPPT is disconnected during the voltage sag.

Control Strategy:

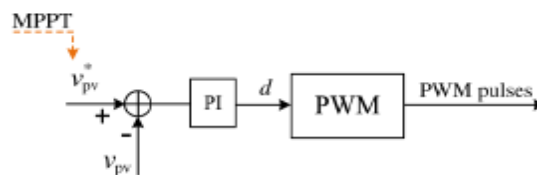


Fig. 10. Control diagram of the dc–dc converter.

In two-stage GCPPPs, the PV voltage ( $v_{pv}$ ) is controlled by the duty cycle ( $d$ ) of the dc–dc converter. The reference for the PV voltage is given by the MPPT, as shown in Fig. 10.

### A. Short-Circuiting the PV Panels

In this method, the dc–dc converter switch is ON ( $d = 1$ ) throughout the voltage sag, as shown in Fig. 11. Consequently, no power is transferred from the PV modules to the dc-link.

Since  $v_{pv}$  is zero, the feed-forward term  $id_{est}$  in (5) defines a fast transition to zero at the beginning of the voltage sag, accelerating the overall dynamic of the controller. Fig. 12 shows some results for an SLG voltage sag with a 60% voltage drop at MV side occurred from  $t = 0.1$  s to  $t = 0.3$  s. The generated power of the PV arrays and also the injected active and reactive power into the grid are shown in Fig. 13. During the voltage sag, the dc-link voltage remains relatively constant,  $id_{ref}$  becomes almost zero with some ripples, and only  $iq_{ref}$  is injected during the fault period. Consequently, the current limiter does not have to be activated in this case. Under unbalanced voltage sags, the output power contains a second-order harmonic [31], which will produce dc-link voltage ripples at the same frequency.

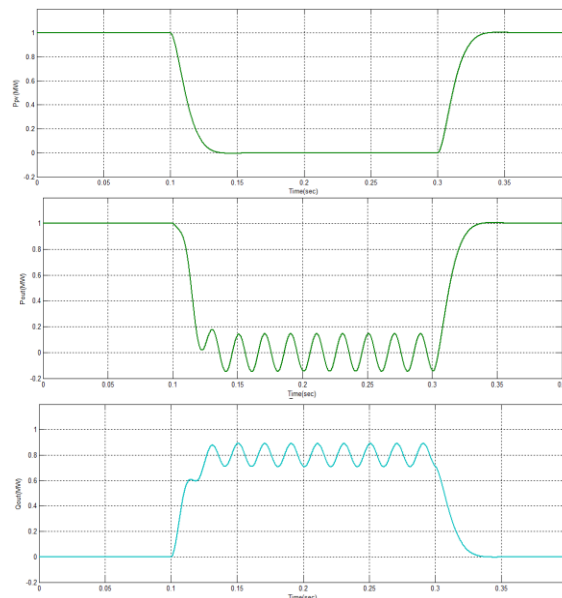


Fig. 13. Short-circuiting the PV panels: (a) overall generated power; (b) injected active power; and (c) reactive power to the grid.

### B. Opening the Circuit of the PV Panels

Another option to avoid transferring power from the PV modules to the dc-link is to keep the dc–dc converter switch OFF throughout the voltage sag ( $d = 0$ ), as shown in Fig. 14. Since, the inverter is not transferring active power into the grid during the voltage sag, the PV voltage  $v_{pv}$  increases until the dc–dc converter inductor is completely discharged ( $i_{pv} = 0$ ).

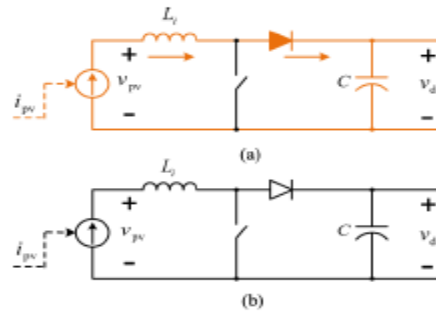


Fig. 14. Current paths in dc–dc converter when turning ON the switch: (a) transition mode and (b) locked in state.

Then, the diode turns OFF and the PV modules stop providing energy into the dc-link [Fig. 14(b)]. This case is similar to the previous one where the diode was continuously ON and no current from the PV was provided to the dc-link. The main difference with the previous case is the transition process, as depicted in Fig. 15.

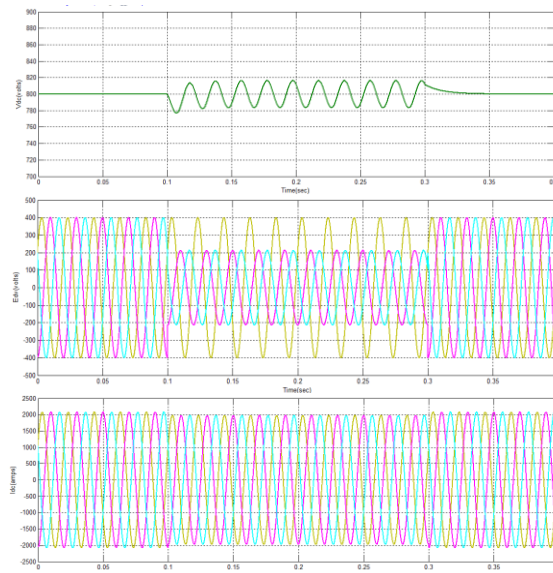


Fig. 15. Turning the dc–dc converter switch ON: (a) grid voltages; (b) grid currents; and (c) dc-link voltage when applying a 60% SLG voltage sag at the MV side.

### C. Injecting Less Power From the PV Panels

In the two previous cases, during the voltage sags, there is no power generated by the PV panels and therefore, only reactive current is injected into the grid. The network operator is allowed to feed the grid through the generating power plant during the voltage sags. For this purpose, the GCPPP is controlled to inject less power into the grid during the voltage sag compared with the pre-fault case, while avoiding overvoltage in the dc-link.

In normal operation, the MPPT function is performed by the dc–dc converter, whereas the dc-link voltage is regulated by the inverter. However, under a voltage sag, some modifications should be implemented in order to keep the GCPPP grid-connected. The proposed method tries to match the power generated by the PV modules with the power injected into the grid while trying to keep the dc-link voltage constant. Unlike the previous cases of keeping the switch ON or OFF during the voltage sag, in this case, power balance is achieved for a value different from zero. Therefore, both active and reactive currents will be injected into the grid.

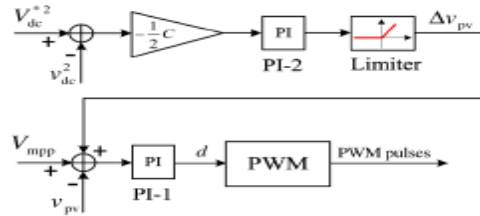


Fig. 17. Adding a controller to the dc–dc converter to force the operating point to move from the MPP to a lower power point.

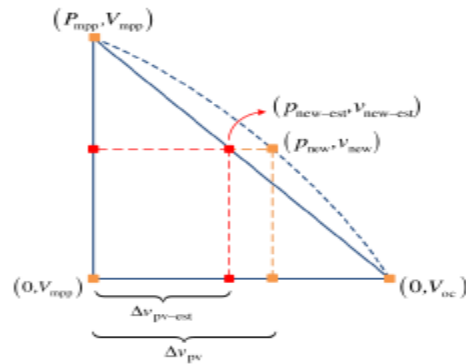


Fig. 18. Triangle used to estimate the new operating point.

The new point  $(p_{new}, v_{new})$  can be estimated by  $(p_{new-est}, v_{new-est})$  on the triangle hypotenuse. According to the Side-Splitter theorem and using interpolation, the estimation of  $v_{new-est}$  is

$$v_{new-est} = \frac{P_{new-est}}{P_{mpp}} (V_{mpp} - V_{oc}) + V_{oc} \quad (7)$$

in which  $P_{mpp}$  and  $V_{mpp}$  represent the pre-fault values at the MPP. The  $p_{new-est}$  can be calculated from the power injected into the grid

$$P_{new-est} \simeq P_{out} = e_d i_d^{ref} \quad (8)$$

$$v_{new-est} = \frac{e_d i_d^{ref}}{P_{mpp}} (V_{mpp} - V_{oc}) + V_{oc} \quad (9)$$

$$\Delta v_{pv-est} = v_{new-est} - V_{mpp} \quad (10)$$

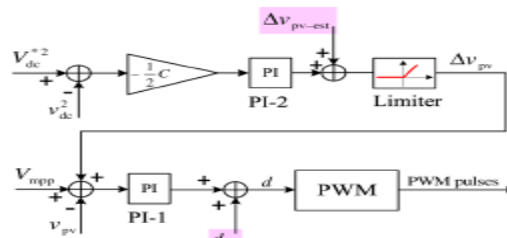


Fig. 19. Updated controller with feed-forward terms to enhance the dynamics of the proposed controller

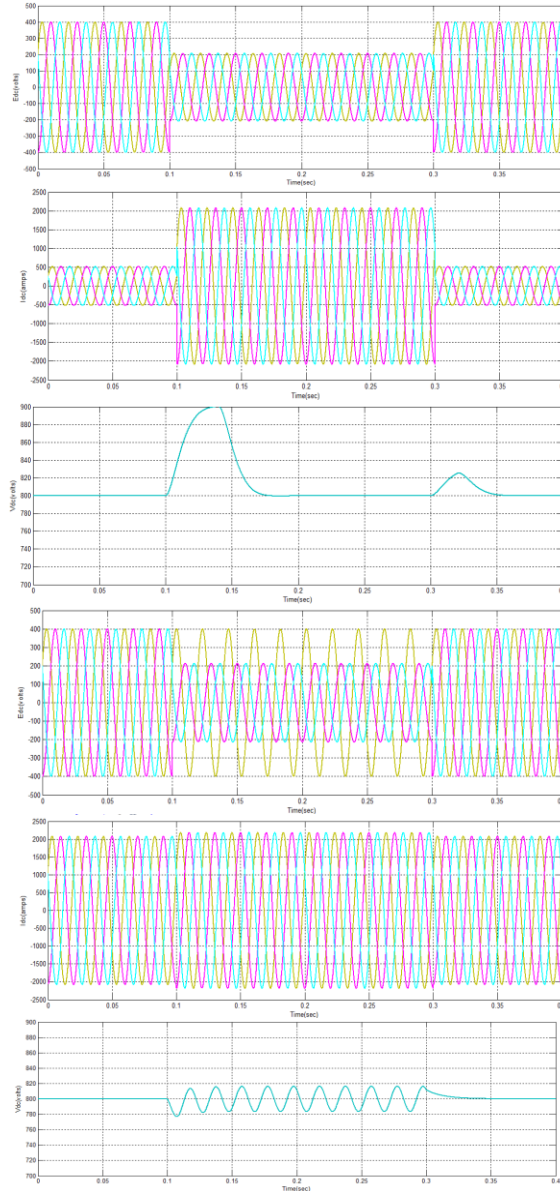
Based on the relationship between the input and the output voltage of the boost dc–dc converter under continuous conduction operating conditions

$$\frac{v_{dc}}{v_{pv}} = \frac{1}{1-d} \quad (11)$$

the estimated duty cycle is

$$d_{est} = 1 - \frac{v_{new-est}}{V_{dc}^*} \quad (12)$$

The updated version of the controller in Fig. 17 is illustrated in Fig. 19, which contains the two feed-forward terms to enhance the dynamics of the proposed controller. The PI controllers PI-1 and PI-2 compensate for the difference between the estimated and the real values of  $d$  and  $\Delta v_{pv}$ , respectively.



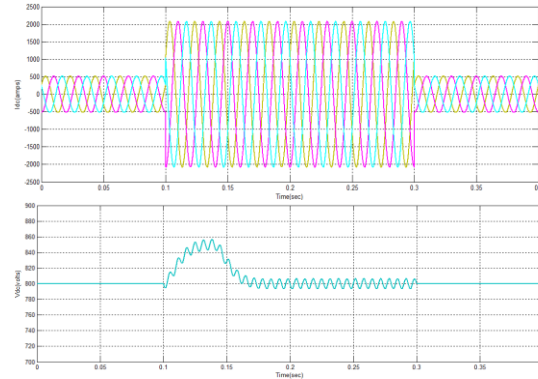


Fig. 21. Control of the dc–dc converter to produce less power under voltage sag: (a) grid voltages under a 3LG with 45% voltage sag at MV side; (b) related grid currents for  $G = 300 \text{ W/m}^2$ ; and (c) related dc-link voltage; (d) grid voltages under an SLG with 65% voltage sag at the MV side; (e) related grid currents for  $G = 1000 \text{ W/m}^2$ ; (f) related dc-link voltage; (g) related grid currents under  $G = 300 \text{ W/m}^2$ ; and (h) related dc-link voltage."

Selected results on the performance of the system under different voltage sags and different solar radiation conditions are shown in Fig. 21. As demonstrated, the output currents always remain balanced during various types of faults and solar radiations and the dynamic performance of the proposed method to reach the new operating point is considerably fast. It should be mentioned that the ripples in the dc-link voltage in Fig. 21(f) and (h) are due to the unbalanced voltage sag.

The preference of the third method, i.e., injecting less power from the PV panels, compared to the first two methods is first due to its capability to inject active power into the grid during the voltage sag to support the grid. Second, it has the capacity to inject balanced currents into the grid even under unbalanced voltage conditions.

#### IV. CONCLUSION

Performance requirements of GCPPPs under fault conditions for single- and two-stage grid-connected inverters have been addressed in this paper. Some modifications have been proposed for controllers to make the GCPPP ride-through compatible to any type of faults according to the GCs. These modifications include applying current limiters and controlling the dc-link voltage by different methods. It is concluded that for the single-stage configuration, the dc-link voltage is naturally limited and therefore, the GCPPP is self-protected, whereas in the two-stage configuration it is not. Three methods have been proposed for the two-stage configuration to make the GCPPP able to withstand any type of faults according to the GCs without being disconnected. The first two methods are based on not generating any power from the PV arrays during the voltage sags, whereas the third method changes the power point of the PV arrays to inject less power into the grid compared with the pre-fault condition. The validity of all the proposed methods to ride-through voltage sags has been demonstrated by multiple case studies performed by simulations

#### REFERENCES

1. Mitra Mirhosseini et al., "Single- and Two-Stage Inverter-Based Grid-Connected Photovoltaic Power Plants With Ride-Through Capability Under Grid Faults" *IEEE Trans. Sustain. Energy*, vol. 2, no. 4, pp. 1-9, Sept. 2014.
2. L. Trilla et al., "Modeling and validation of DFIG 3-MW wind turbine using field test data of balanced and unbalanced voltage sags," *IEEE Trans. Sustain. Energy*, vol. 2, no. 4, pp. 509–519, Oct. 2011.
3. M. Popat, B. Wu, and N. Zargari, "Fault ride-through capability of cascaded current-source converter-based offshore wind farm," *IEEE Trans. Sustain. Energy*, vol. 4, no. 2, pp. 314–323, Apr. 2013.
4. A. Marinopoulos et al., "Grid integration aspects of large solar PV installations: LVRT capability and reactive power/voltage support requirements," in *Proc. IEEE Trondheim PowerTech*, Jun. 2011, pp. 1–8.

5. G. Islam, A. Al-Durra, S. M. Muyeen, and J. Tamura, "Low voltage ride through capability enhancement of grid connected large scale photovoltaic system," in *Proc. 37th Annu. Conf. IEEE Ind. Electron. Soc. (IECON)*, Nov. 2011, pp. 884–889.
6. P. Dash and M. Kazerani, "Dynamic modeling and performance analysis of a grid-connected current-source inverter-based photovoltaic system," *IEEE Trans. Sustain. Energy*, vol. 2, no. 4, pp. 443–450, Oct. 2011.
7. A. Yazdani et al., "Modeling guidelines and a benchmark for power system simulation studies of three-phase single-stage photovoltaic systems," *IEEE Trans. Power Del.*, vol. 26, no. 2, pp. 1247–1264, Apr. 2011.
8. A. Radwan and Y.-R. Mohamed, "Analysis and active suppression of acand dc-side instabilities in grid-connected current-source converter-based photovoltaic system," *IEEE Trans. Sustain. Energy*, vol. 4, no. 3, pp. 630–642, Jul. 2013.
9. J. Miret, M. Castilla, A. Camacho, L. Garcia de Vicuna, and J. Matas, "Control scheme for photovoltaic three-phase inverters to minimize peak currents during unbalanced grid-voltage sags," *IEEE Trans. Power Electron.*, vol. 27, no. 10, pp. 4262–4271, Oct. 2012.
10. G. Azevedo, P. Rodriguez, M. Cavalcanti, G. Vazquez, and F. Neves, "New control strategy to allow the photovoltaic systems operation under grid faults," in *Proc. Brazilian Power Electron. Conf. (COBEP)*, Sep. 2009, pp. 196–201.